

InnoAds-Composer: Efficient Condition Composition for E-Commerce Poster Generation

Yuxin Qin^{1*}, Ke Cao^{1*}, Haowei Liu^{2*}, Ao Ma^{1†}, Fengheng Li¹, Honghe Zhu¹, Zheng Zhang^{1‡}, Run Ling¹, Wei Feng¹, Xuanhua He³, Zhanjie Zhang^{4‡}, Zhen Guo¹, Haoyi Bian¹, Jingjing Lv¹, Junjie Shen¹, Ching Law¹

¹JD.com, Inc., Beijing, China

²Chongqing University of Posts and Telecommunications, Chongqing, China

³The Hong Kong University of Science and Technology, Hong Kong, China

⁴Zhejiang University, Hangzhou, China

miao.8@jd.com, zhangzhanj@126.com



Figure 1. Inno-Composer generates high-quality e-commerce posters under three independent controls—background style, subject appearance, and glyph text. Each row varies a single condition while keeping the other two fixed. The bottom-right inset shows the input of the varied condition.

Abstract

E-commerce product poster generation aims to automatically synthesize a single image that effectively conveys product information by presenting a subject, text, and a designed style. Recent diffusion models with fine-grained and efficient controllability have advanced product poster synthesis, yet they typically rely on multi-stage pipelines, and simultaneous control over subject, text, and style re-

mains underexplored. Such naive multi-stage pipelines also show three issues: poor subject fidelity, inaccurate text, and inconsistent style. To address these issues, we propose InnoAds-Composer, a single-stage framework that enables efficient tri-conditional control tokens over subject, glyph, and style. To alleviate the quadratic overhead introduced by naive tri-conditional token concatenation, we perform importance analysis over layers and timesteps and route each condition only to the most responsive positions, thereby shortening the active token sequence. Besides, to improve the accuracy of Chinese text rendering, we design a Text Feature Enhancement Module (TFEM) that integrates fea-

* Equal contribution.

† Project leader.

‡ Corresponding author.

tures from both glyph images and glyph crops. To support training and evaluation, we also construct a high-quality e-commerce product poster dataset and benchmark, which is the first dataset that jointly contains subject, text, and style conditions. Extensive experiments demonstrate that InnoAds-Composer significantly outperforms existing product poster methods without obviously increasing inference latency.

1. Introduction

E-commerce product poster generation has emerged as a crucial task that aims to automatically synthesize a single image effectively conveying product information through the integration of subject, text, and a designed style. Recently, diffusion models [11, 13, 16, 21, 28, 32, 37, 44, 47, 48, 50, 56, 57, 75, 82, 83] have demonstrated fine-grained and efficient control over image synthesis, achieving high visual fidelity and semantic richness, which has greatly promoted the development of automated poster design. However, e-commerce poster generation remains relatively underexplored. Unlike free-form artistic layouts, retail posters must follow strict layout and branding rules while maintaining subject fidelity, style consistency, and text accuracy, making poster creation a constrained and multi-objective problem.

Current e-commerce poster generation systems still fall short in three respects. First, most do not offer end-to-end joint control of background style, subject fidelity, and text accuracy within a single model; multi-stage pipelines [7, 17] that compose the scene and render the text tend to be inaccurate, resulting in style inconsistency and loss of subject fidelity. Second, emerging single-stage approaches [8, 38] incorporate text control but struggle to render complex scripts and small glyphs with high fidelity. Third, the designed background style is often prompt-driven and may deviate from global style or semantic constraints [18, 72, 77, 79, 80]. These limitations are exacerbated by the scarcity of training data: e-commerce poster datasets with fine-grained, multi-condition annotations are limited, hindering the learning of reliable design priors and robust controllability.

To address these challenges, we introduce InnoAds-Composer, a single-stage, multi-condition framework for e-commerce poster synthesis built on an MM-DiT backbone. A unified tokenization maps style, subject, and glyph conditions into the same token space, enabling joint inference while preserving the priors of the underlying text-to-image model. To remedy the weakness of text rendering, we propose a Text Feature Enhancement Module (TFEM): one branch encodes the entire glyph image with a VAE to obtain visual glyph tokens; a second branch processes single-glyph crops with an OCR backbone and injects multi-positional

cues (absolute location, font size, and local position). For the above single/entire glyph tokens, we use a lightweight character encoder and then fuse them, improving glyph sharpness, boundary integrity, and readability in a principled way. To curb computation and avoid redundant conditioning, we conduct layer and timestep importance analysis, estimating the backbone’s importance differences for the three conditions and performing importance-aware injection. By retaining each condition only at its most responsive layers and diffusion steps, we shorten the effective sequence and temper the quadratic growth of attention. In implementation, a decoupled attention design preserves the main stream’s sensitivity to conditions while removing costly, low-value interactions, yielding consistent efficiency gains in both training and inference. To support training and evaluation, we also create a high-quality e-commerce poster dataset and benchmark. This data pipeline is designed to provide diverse background style control, along with accurate subject and glyph controls, providing the supervision needed for robust multi-condition generation. Qualitative results in Figure 1 show that InnoAds-Composer produces high-quality posters under three independent controls.

Our contributions can be summarized as follows:

- We propose InnoAds-Composer, a single-stage framework for e-commerce posters that provides efficient, coordinated control over style, subject, and text. With TFEM, the model fuses entire glyph and single glyph features augmented by positional cues, systematically improving text accuracy.
- We reveal non-uniform and complementary patterns of condition influence across layer and timestep, and leverage these differences to inject tokens only at the most responsive layers and steps, reducing the activated token sequence and restraining attention’s quadratic complexity growth.
- We design a new data construction pipeline and release InnoComposer-80K together with InnoComposer-Bench, covering subject, glyph, style, and overall quality, enabling unified comparison for e-commerce poster generation.
- Extensive experiments show that our method effectively addresses the core difficulties of e-commerce poster generation, achieving strong visual quality and control while significantly lowering inference cost.

2. Related Work

Please see Appendix Sec. 1.

3. Datasets and Benchmark

As shown in Figure 2, we construct a high-quality bilingual e-commerce poster dataset through a structured pipeline. The left panel presents typical cases composed of three

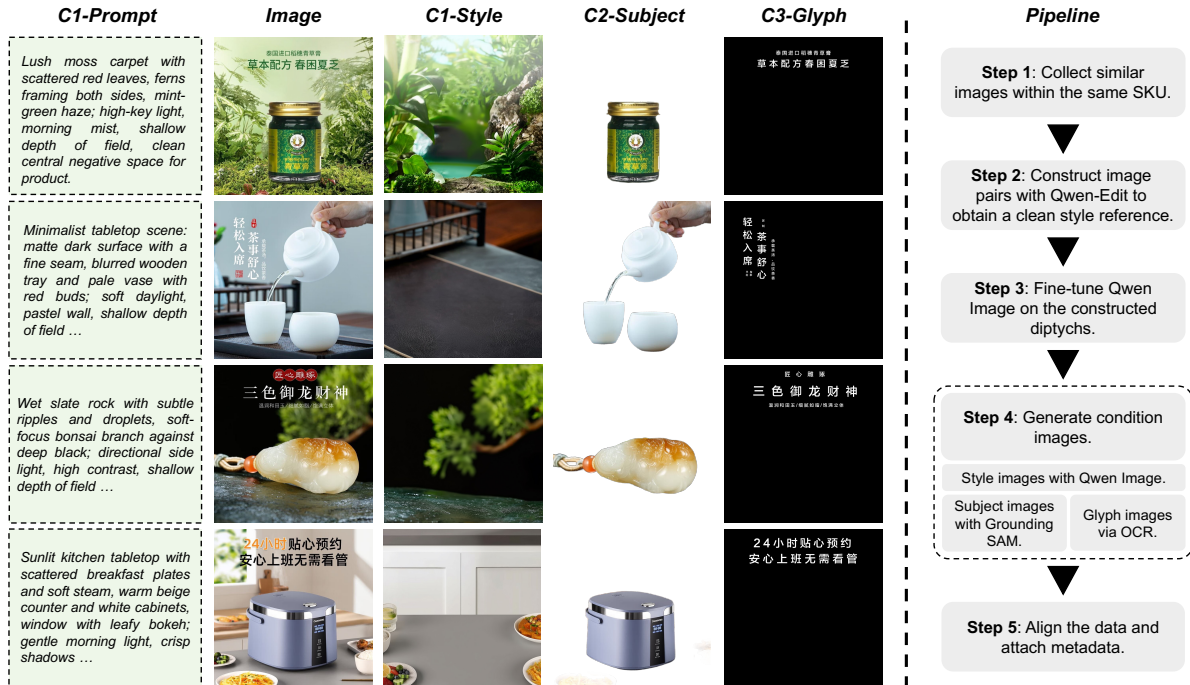


Figure 2. Case Examples and Dataset Construction Pipeline for E-commerce Poster Generation.

customized inputs: a background-style image that conveys global aesthetics and background elements, a subject image that specifies the product and its approximate location, and a glyph image that provides the textual content to be rendered. The right panel summarizes the pipeline. Images are first grouped by Stock Keeping Unit (SKU), a unique identifier for each distinct product, and annotators select visually similar pairs within each group. For one image in each pair, Qwen-Edit [63] removes product content to obtain a clean style reference; when needed, a super-resolution model improves clarity. The reference and its paired image are concatenated into a diptych, and the reference side is recorded. These diptychs then supervise a fine-tuning of Qwen-Image [63] so the generator learns to produce style-consistent counterparts, yielding clean background references. Using the fine-tuned generator, we synthesize style images in batches. Unlike conventional pipelines that enforce a tight pixel-level match between the content image and its style counterpart, our synthesized backgrounds are semantically aligned yet intentionally differ in local details, which fosters diversity during generation. The Glyph images containing both Chinese and English are extracted from the original images through OCR, and subject images are obtained by segmenting the product with Grounded-SAM [43, 61] to produce foregrounds or masks. Finally, we curate the data, perform de-duplication and resolution normalization, and record metadata such as SKU and pre-processing parameters. Following this pipeline, we construct InnoComposer-80K, a corpus of 80,000 poster sam-

ples. Each sample contains a text prompt, a subject image, a background-style image, and a glyph image, providing comprehensive supervision for multi-condition poster generation. For evaluation, we curate InnoComposer-Bench, a 300-item subset ranked by product emphasis, style consistency, and text accuracy; these items are strictly held out from training to ensure fair comparison across methods.

4. Methods

4.1. InnoAds-Composer

Figure 3 illustrates InnoAds-Composer, a multi-condition, text-to-image advertising framework built on an MM-DiT backbone. A user prompt is first processed by a pretrained T5 text encoder, which tokenizes and embeds the prompt into a sequence of text tokens h^p . In parallel, a reference image is mapped by the VAE encoder into a latent representation h^z , which is then partitioned into patches to form a set of visual tokens. The text and visual tokens are unified and propagated through MM-Attention blocks that interleave intra-modal self-attention with cross-modal interactions. This design aligns language semantics with fine-grained visual structure, enabling precise control over the generated content.

To meet e-commerce requirements that require creatives to honor product focus, layout constraints, brand elements, and style specifications, InnoAds-Composer accepts multiple heterogeneous conditions, such as product attributes, layout hints, brand text or logos, and stylistic tags. These

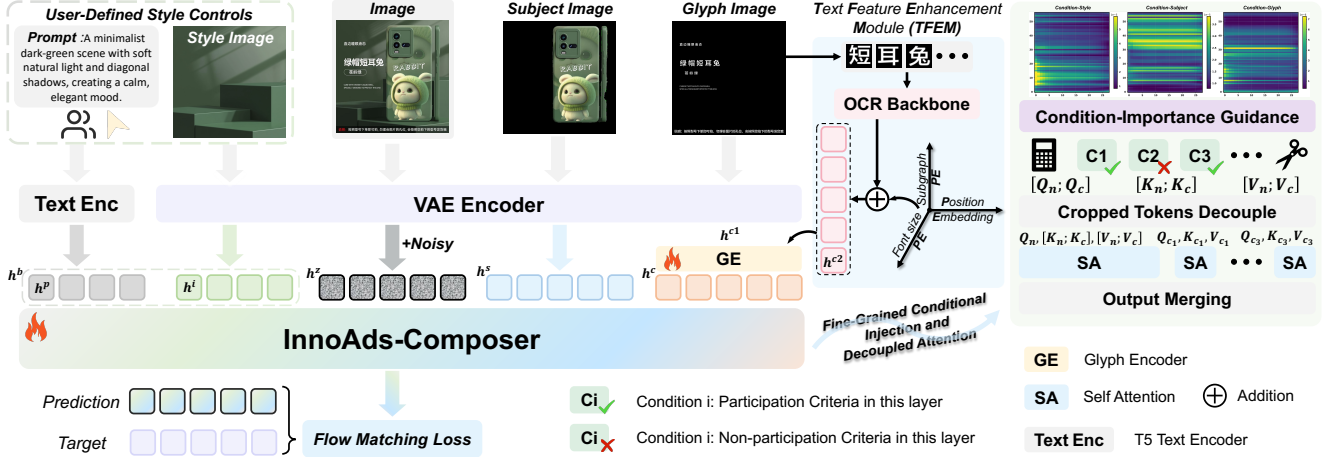


Figure 3. **Overview of InnoAds-Composer.** The framework comprises three modules: (1) *Multi-Condition Tokenization*, which maps heterogeneous controls into a shared token space and aligns them with the MM-DiT backbone; (2) *Importance-Aware Condition Injection*, which routes each control to its importance layers to improve efficiency while preserving controllability; and (3) *Decoupled Attention*, which allows the main stream to attend to condition cues while the condition branch performs self-attention only, removing the extra path to reduce cost and maintain training–inference consistency.

conditions are embedded in the same token space and injected across MM-DiT layers, guiding generation while preserving the strong priors of the underlying text-to-image model. Operating end-to-end in the latent space, the system maintains the image quality and diversity of the base model and delivers high-fidelity, efficiently controllable poster synthesis tailored to e-commerce use cases.

4.1.1. Multi-Condition Tokenization

To enable high-quality, controllable e-commerce poster generation, InnoAds-Composer adopts a unified multi-condition tokenization strategy. Heterogeneous controls, including global background style, subject imagery, and text layout, are mapped to a shared embedding space and injected across MM-DiT through MM-Attention, preserving the base T2I model’s priors while enabling precise end-to-end control.

User-Defined Background Style Control. Global style is specified either by a style prompt or by a style image, handled within a single formulation. Pretrained text encoder tokenizes the prompt into text tokens h^p , whereas a style image is encoded by a VAE into a latent grid and patchified into visual tokens h^i . The resulting background-style tokens are defined as:

$$h^b = \begin{cases} \mathcal{C}(h^p), & m = 0 \\ \mathcal{C}(h^i, h^{p0}), & m = 1. \end{cases} \quad (1)$$

where $m = 1$ indicates the presence of a style image, \mathcal{C} represents the concatenation. h^{p0} is a fixed anchor prompt independent of user inputs;

Subject Control. To emphasize the product foreground and suppress background leakage, regions outside the sub-

ject are filled with black to form an explicit mask. The masked image is then encoded by the VAE and patchified, producing subject tokens h^s that capture the object’s structure and appearance while remaining aligned to the shared token space.

Glyph Control with Text-Feature Enhancement. Readable, well-placed text is pivotal for conversion in ad creatives. We therefore introduce a dual-branch glyph control with a Text Feature Enhancement Module (TFEM). In the first branch, the entire glyph image is encoded by a VAE and patchified to produce visual glyph tokens h^{c1} . In the second branch, single-glyph crops extracted from the original glyph image are first processed by an OCR backbone; afterward, three positional encodings are added: the absolute position in the original image, a font-size code indicating the intended scale, and a local positional encoding within each crop, yielding h^{c2} . A lightweight Character Encoder then fuses both sources:

$$h^c = \text{GlyphEnc}(h^{c1}, h^{c2}) \quad (2)$$

yielding glyph tokens that jointly encode glyph fidelity, encompassing clarity and edge integrity, together with semantic and positional intent expressed through legibility and alignment.

4.1.2. Importance-Aware Condition Injection

Building on multi-condition tokenization, we estimate the MM-DiT backbone’s preferences for background, subject, and character conditions across layers and diffusion timesteps in Sec . 4.2. The resulting preference curves indicate where each condition exerts the strongest influence. Guided by these curves and validated through ablation, we

retain by default 40% of style tokens, 50% of subject tokens, and 20% of glyph tokens. In any layer selected for condition type i , the corresponding condition tokens are concatenated with the main-stream noisy-latent tokens h^z , and all non-selected condition tokens are omitted at that layer. This targeted scheduling shortens the active sequence per layer and substantially curbs token-induced computational growth in MM-DiT, while preserving precise controllability.

4.1.3. Decoupled Attention

In token-based conditional diffusion processes, condition tokens generally evolve slowly across timesteps and their representations remain largely unaffected by the noisy latent tokens [4, 22, 23, 58]. Applying full attention over the concatenated sequence $[\mathbf{h}_n; \mathbf{h}_c]$ therefore incurs redundant computation, as it repeatedly processes interactions that are either nearly static across steps or provide minimal useful signal relative to their computational cost.

We address this by removing the pathway from condition queries to noisy-latent keys while retaining the pathway from noisy-latent queries to condition keys. Conditions continue to guide generation through the mainstream, and the condition branch no longer follows rapidly changing noise. Let $\mathbf{Q}_n, \mathbf{K}_n, \mathbf{V}_n$ be the queries, keys, and values of the noisy-latent tokens h^z , and $\mathbf{Q}_{ci}, \mathbf{K}_{ci}, \mathbf{V}_{ci}$ those of condition type i . We compute

$$O_n = \text{Attn}(\mathbf{Q}_n, [\mathbf{K}_n; \mathbf{K}_{ci}], [\mathbf{V}_n; \mathbf{V}_{ci}]) \quad (3)$$

$$O_{ci} = \text{Attn}(\mathbf{Q}_c, \mathbf{K}_{ci}, \mathbf{V}_{ci}) \quad (4)$$

$$O = [O_n, O_{ci}] \quad (5)$$

The main stream attends to both its own context and the condition cues, whereas the condition stream performs self-attention only. This eliminates the $\mathbf{Q}_c\text{-}\mathbf{K}_n$ cross-attention term during both training and inference, reducing computation while preserving consistency. Moreover, since the condition stream no longer depends on the timestep, its activations at each block can be computed once and cached for reuse across all timesteps during inference.

4.1.4. Two-Stage Training Strategy

Concatenating multiple condition tokens inflates the sequence length and, in turn, the attention cost. To control complexity, we prune tokens guided by condition-importance analysis and adopt a two-stage training. In Stage I, all condition tokens are retained to train a fully conditioned poster generator. In Stage II, we remove the selected tokens and fine-tune the network. During this phase, diffusion timesteps are sampled in proportion to their mass in the global importance map, thereby aligning the training emphasis with the importance distribution observed at evaluation. This procedure mitigates the performance drop from pruning, preserves the generative capacity of the full model, and substantially reduces inference-time computation.

4.2. Conditions Importance Analysis

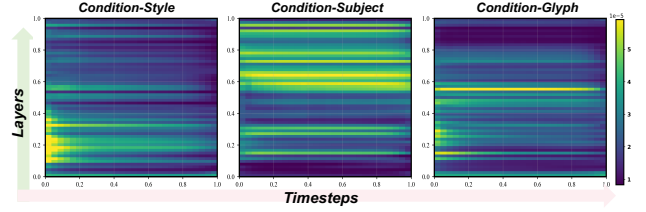


Figure 4. The importance heatmaps of the three conditions across timesteps and layers.

Self-attention in transformers typically dominates both computational cost [2, 26] and memory usage [5, 27, 69] due to its quadratic complexity [6]. In MM-DiT, this issue is further amplified by the concatenation of condition tokens with noisy-latent tokens, significantly increasing the sequence length and exacerbating the computational bottleneck. Specifically, in e-commerce poster generation, the introduction of diverse conditions such as reference images, subject representations, and text content offers precise control over the overall style, product depiction, and text clarity. However, this increased flexibility comes at a high computational cost, particularly when these conditions are uniformly injected across all layers and timesteps of the model. To address this challenge, we conduct a detailed analysis of the importance of different control conditions across various layers and timesteps in MM-DiT. By investigating how each condition influences the generation process at different stages, we identify the most effective layers and timesteps for injecting each condition. This allows us to determine where each condition has the most significant impact and where it can be omitted to improve computational efficiency. Based on these insights, we propose a selective injection strategy. In this strategy, each condition is routed only to its most relevant layers and timesteps, while less responsive conditions are omitted. This selective injection ensures an efficient allocation of computational resources, balancing high-quality generation with reduced computational load.

To validate this approach, we first trained a model that incorporates the full set of control conditions, with B layers and T total diffusion steps. When all control conditions are included, the input sequence is represented as $h^{total} = [h^p, h^z, h^i, h^s, h^c]$, with the total sequence length given by $l^{tot} = l^p + l^z + l^i + l^s + l^c$. At each timestep $t \in 1, \dots, T$ and layer $b \in 1, \dots, B$, the input to the multi-head attention mechanism consists of queries and keys, denoted as $Q^{(b,t)}$ and $K^{(b,t)} \in \mathbb{R}^{h \times l^{tot} \times d}$. We then measure the importance of the three visual input conditions through attention preference weights:

$$A^{(b,t)} = \text{Softmax}\left(\frac{Q^{(b,t)}, K^{(b,t)\top}}{\sqrt{d}}\right) \in \mathbb{R}^{h \times l^{tot} \times l^{tot}} \quad (6)$$



Figure 5. Qualitative results. **Left:** Input conditions, including C1-style images, C2-glyph images, and C3-subject images. **Right:** Results generated by different methods.

For each control condition ci , we extract its corresponding subgraph, apply the relevant condition mask, and compute the full-dimensional mean to obtain a scalar value for each timestep and layer:

$$S_{ci}(b, t) = \text{Mean}(A^{b,t,c} \odot \text{mask}_{ci}) \quad (7)$$

Here, the mask for the subject condition is applied to all areas outside the subject in the image, while the mask for the glyph condition covers regions outside the textual content.

Figure 4 illustrates the final visualization, showing the importance heatmaps of the three conditions across different timesteps and layer positions. From these maps, we observe that the background style dominates in the early layers and early timesteps but decays rapidly as the generation progresses. In contrast, the subject condition forms a persistent high-intensity band in the mid-to-deep layers, spanning most of the timesteps. The glyph condition, while exhibiting a lower overall magnitude, gradually increases in intensity in the middle layers and later timesteps, corresponding to the refinement of strokes and glyphs. Overall, the conditions display a non-uniform and complementary relationship across both timesteps and model depth. This analysis allows us to refine the selective injection strategy, ensuring that attention computations are retained for conditions with higher importance in $S_{ci}(b, t)$, while skipping less responsive locations, thus optimizing the overall efficiency of the model.

5. Experiments

5.1. Settings

Implementation Details. Please see Appendix Sec. 2.

Comparative Methods. Since our approach is a multi-conditional generative method, we compare it not only with the open-source base model Flux [28] and its variants, but also with state-of-the-art models across several relevant categories, including visual text generation, conditional image generation, and closed-source commercial models. Specifically, for visual text generation, we select Glyph-ByT5-v2 [34] and AnyText2 [54] as comparison baselines. For conditional image generation, we include Flux-Kontext [28], OminiControl2 [52], OminiGen2 [64], the subject-driven USO [65], and the poster generation model PosterMaker [18]. In addition, we also incorporate an image generation foundation model Qwen-Image-Edit [62] and a closed-source commercial model Seedream 4.0 [45], as part of the comparison.

Evaluation Metrics. Following previous works, we adopt multiple quantitative metrics to evaluate different aspects of our generated results, including visual text quality, subject consistency, background style consistency, and general image quality. Specifically, Sentence Accuracy (Sen. Acc) and Normalized Edit Distance (NED) are used to assess the accuracy of visual text generation within images. For subject consistency, we employ DINO score and IoU, where the subject regions are first extracted using Grounded SAM [43], and the DINO score is computed as the cosine similarity between the generated and reference subject features in the DINO embedding space, while IoU measures their spatial overlap. To evaluate background style consistency, we use CSD [46] and CLIP-I, where CLIP-I represents the cosine similarity between generated and reference images in the CLIP embedding space, capturing global background similarity. Finally, IR-Score [68] and FID are

Table 1. Quantitative results. The best scores are **bolded**, while the second-best is underlined. Models marked with “*” in the table indicate closed-source models, while “-” denotes that the corresponding metric cannot be computed for the images generated by that model.

Models	Visual Text Quality		Subject Consistency		Style Consistency		General Quality	
	Sen. Acc \uparrow	NED \uparrow	DINO \uparrow	IoU \uparrow	CSD \uparrow	CLIP-I \uparrow	IR-Score \uparrow	FID \downarrow
Flux-inpaint [28]	-	-	0.853	0.877	-	-	0.822	79.41
Flux-Fill [28]	-	-	0.867	0.932	-	-	0.950	75.12
Flux-Kontext [28]	-	-	0.831	0.793	0.573	0.470	0.955	76.76
OmniControl2 [52]	-	-	0.812	0.685	0.692	0.477	0.930	80.13
OmniGen2 [64]	-	-	0.820	0.822	0.685	0.433	0.945	81.83
USO [65]	-	-	0.900	0.727	0.719	0.577	0.911	74.19
Glyph-ByT5-v2 [34]	0.685	0.815	-	-	-	-	0.837	82.63
Anytext2 [54]	0.721	0.582	-	-	-	-	0.701	86.35
PosterMaker [18]	0.765	0.848	0.916	0.954	-	-	0.974	60.55
Flux-Text & inpaint [28]	0.775	0.892	0.893	0.824	-	-	0.956	73.71
Qwen-Image-Edit [62]	0.831	0.960	<u>0.922</u>	0.903	0.722	0.660	0.994	69.86
Seedream 4.0* [45]	0.865	<u>0.972</u>	0.864	0.837	0.700	<u>0.639</u>	<u>1.012</u>	64.21
Ours (Stage I)	<u>0.857</u>	0.976	0.923	0.972	0.729	<u>0.582</u>	1.036	54.39
Ours (Stage II)	<u>0.847</u>	0.969	0.914	<u>0.960</u>	<u>0.727</u>	0.594	0.995	<u>55.24</u>

adopted to assess the overall perceptual fidelity and distributional quality of the generated images.

5.2. Qualitative Analyses

As shown in Fig. 5, the baseline models exhibit clear limitations when applied to the task of product poster generation. Flux-Fill and USO can only perform image synthesis driven by either a subject reference or both subject and background reference images, respectively, but neither is capable of generating images containing visual text, making them unsuitable for poster creation scenarios that require integrated textual elements. PosterMaker, while capable of generating images with both the specified subject and embedded text, struggles to maintain background style consistency, often failing to reproduce the desired stylistic characteristics of product posters.

In contrast, Qwen-Image-Edit and Seedream 4.0 demonstrate relatively good subject consistency and visual text rendering capabilities. Nonetheless, they often produce redundant or mismatched text, and their style transfer tends to exhibit a “copy-and-paste” effect, failing to generate diverse or contextually coherent backgrounds based on the style images. Our proposed InnoAds-Composer effectively overcomes these limitations, achieving strong consistency across text, subject, and background style. It is capable of generating visually appealing, semantically coherent, and stylistically controlled poster images, demonstrating its practicality for multi-conditional product advertisement generation.

5.3. Quantitative Evaluations

Table 1 presents the quantitative comparison across all baselines and our proposed InnoAds-Composer under two configurations, Stage I and Stage II. Overall, in Stage I, our method achieves the best performance in nearly all aspects. It obtains the highest Sen. Acc of 0.857 and NED of 0.976, indicating superior visual text generation quality. In terms of subject consistency, it also leads with a DINO score of 0.923 and an IoU of 0.972, demonstrating strong alignment between the generated subjects and their references. For background style consistency, it attains a CSD of 0.729 and a CLIP-I score of 0.582, showing stable preservation of scene style. Moreover, it achieves the best overall image quality, reflected by an IR-Score of 1.036 and a FID of 54.39, significantly outperforming all open-source and commercial competitors. After Stage II, our method maintains comparable performance while improving computational efficiency. By performing importance analysis across layers and timesteps and routing each condition only to its most responsive regions, Stage II effectively shortens the active token sequence and curbs quadratic compute growth. Although it shows a slight decline in most metrics, its overall quality remains competitive, achieving a Sen. Acc of 0.847, DINO score of 0.914, and FID of 55.24. This balance between accuracy and efficiency highlights the scalability and practicality of the proposed multi-conditional generation framework.

We further evaluate the computational efficiency of our method in terms of inference latency, FLOPs, and GPU memory consumption, as summarized in Table 2. Leveraging decoupled attention, Stage I reduces latency by 26.5%

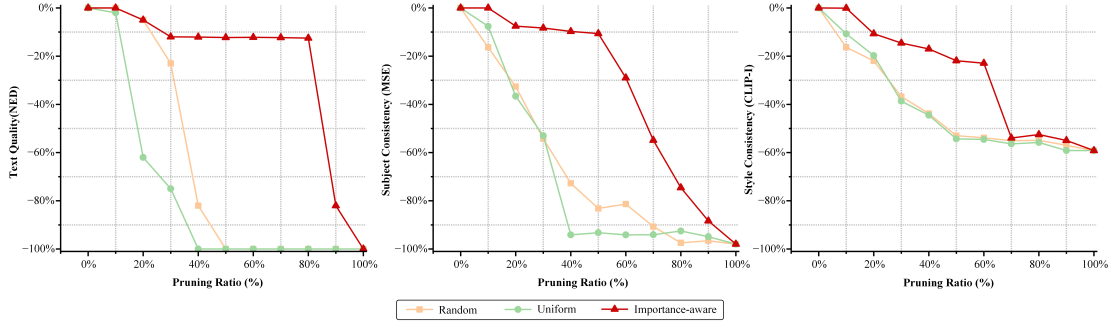


Figure 6. Comparison of image generation quality under different condition token pruning strategies.

Table 2. Efficiency analysis across different training stages.

Methods	Latency(s)	FLOPs(T)	Memery(G)
Flux-Kontext [28]	76.02	218.45	55.29
Ours (Stage I)	55.87	165.56	39.71
Ours (Stage II)	47.32	135.25	39.41

and FLOPs by 24.2% compared to Flux-Kontext (which uses native full attention), with notably lower memory usage. Stage II builds on this by pruning redundant tokens and applying adaptive fine-tuning, achieving further reductions of 37.8% in latency and 38.1% in FLOPs—without compromising generation quality. These results demonstrate that our combined decoupled attention and token pruning strategy significantly improves efficiency while maintaining high-quality output, striking a strong balance between performance and resource usage.

5.4. Ablation Study

Effect of Text Feature Enhancement Module. As shown in Fig. 7, we conduct an ablation study on the Text Feature Enhancement Module. Without this module, the generated images exhibit noticeable textual errors, whereas incorporating it significantly improves the quality and accuracy of rendered text. Quantitatively, introducing the Text Feature Enhancement Module leads to an approximate 5% improvement in Sen. Acc, demonstrating its effectiveness in enhancing visual text generation.

Analyses of Importance-aware Condition Injection. After the first-stage training, we evaluate three condition token pruning strategies during inference: random, uniform, and importance-aware. Generation quality is assessed using NED for text quality, MSE for subject consistency, and CLIP-I for style consistency. As shown in Fig. 6, random and uniform pruning cause a rapid decline across all metrics, while the importance-aware strategy maintains stable quality until a large portion of uninformative tokens is removed. Specifically, glyph quality remains robust until about 80% of tokens are pruned, and subject and style conditions preserve good performance up to roughly 50% and



Figure 7. Ablation study of Text Feature Enhancement Module. Zoom in for details.

60% pruning, respectively, before a sharp degradation occurs. Therefore, we adopt the importance-aware condition injection strategy and apply the corresponding token pruning ratios during the second-stage training to effectively reduce computational overhead.

6. Conclusion

We presented InnoAds-Composer, a single-stage, multi-condition framework for e-commerce poster generation that delivers simultaneously subject, text, and designed style. By unifying subject, style, and glyph (text) tokens in the same space and preserving the priors of an MM-DiT backbone, our approach enables joint inference without multi-stage pipelines. The proposed Text Feature Enhancement Module (TFEM) fuses single/entire glyphs with positional information, substantially improving text’s sharpness, boundary integrity, and readability. Complementing this, we perform importance-aware condition injection and decoupled attention to reduce redundant interactions and shorten the activated sequence, leading to improved inference efficiency. To facilitate learning and fair comparison, we constructed InnoComposer-80K and the evaluation benchmark InnoComposer-Bench, covering subject, text, style, and overall quality.

References

- [1] Sotiris Anagnostidis, Gregor Bachmann, Yeongmin Kim, Jonas Kohler, Markos Georgopoulos, Artsiom Sanakoyeu, Yuming Du, Albert Pumarola, Ali Thabet, and Edgar Schönfeld. Flexidit: Your diffusion transformer can easily generate high-quality samples with less compute. In *Proceedings of the Computer Vision and Pattern Recognition Conference*, pages 28316–28326, 2025. 1
- [2] Xiuli Bi, Haowei Liu, Weisheng Li, Bo Liu, and Bin Xiao. Using my artistic style? you must obtain my authorization. In *European Conference on Computer Vision*, pages 305–321. Springer, 2024. 5
- [3] Xiuli Bi, Jian Lu, Bo Liu, Xiaodong Cun, Yong Zhang, Weisheng Li, and Bin Xiao. Customttt: Motion and appearance customized video generation via test-time training. In *Proceedings of the AAAI Conference on Artificial Intelligence*, pages 1871–1879, 2025. 1
- [4] Ke Cao, Xuanhua He, Tao Hu, Chengjun Xie, Jie Zhang, Man Zhou, and Danfeng Hong. Shuffle mamba: State space models with random shuffle for multi-modal image fusion. *arXiv preprint arXiv:2409.01728*, 2024. 5
- [5] Ke Cao, Xuanhua He, Keyu Yan, Tao Hu, Rui Li, Chengjun Xie, and Jie Zhang. Frequency decomposition-driven network for jpeg artifacts removal. In *2024 IEEE International Conference on Multimedia and Expo (ICME)*, pages 1–6. IEEE, 2024. 5
- [6] Ke Cao, Jing Wang, Ao Ma, Jiasong Feng, Zhanjie Zhang, Xuanhua He, Shanyuan Liu, Bo Cheng, Dawei Leng, Yuhui Yin, et al. Relactrl: Relevance-guided efficient control for diffusion transformers. *arXiv preprint arXiv:2502.14377*, 2025. 5
- [7] Tingfeng Cao, Junsheng Kong, Xue Zhao, Wenqing Yao, Junwei Ding, Jinhui Zhu, and Jiandong Zhang. Product2img: Prompt-free e-commerce product background generation with diffusion model and self-improved lmm. In *Proceedings of the 32nd ACM International Conference on Multimedia*, pages 10774–10783, 2024. 2
- [8] Haoxing Chen, Zhuoer Xu, Zhangxuan Gu, Yaohui Li, Changhua Meng, Huijia Zhu, Weiqiang Wang, et al. Diffute: Universal text editing diffusion model. *Advances in Neural Information Processing Systems*, 36:63062–63074, 2023. 2
- [9] Haoyu Chen, Xiaojie Xu, Wenbo Li, Jingjing Ren, Tian Ye, Songhua Liu, Ying-Cong Chen, Lei Zhu, and Xinchao Wang. Posta: A go-to framework for customized artistic poster generation. In *Proceedings of the Computer Vision and Pattern Recognition Conference*, pages 28694–28704, 2025. 1
- [10] Jingye Chen, Yupan Huang, Tengchao Lv, Lei Cui, Qifeng Chen, and Furu Wei. Textdiffuser: Diffusion models as text painters. *Advances in Neural Information Processing Systems*, 36:9353–9387, 2023. 1
- [11] Junsong Chen, Jincheng Yu, Chongjian Ge, Lewei Yao, Enze Xie, Yue Wu, Zhongdao Wang, James Kwok, Ping Luo, Huchuan Lu, et al. Pixart- α : Fast training of diffusion transformer for photorealistic text-to-image synthesis. *arXiv preprint arXiv:2310.00426*, 2023. 2
- [12] Jingye Chen, Yupan Huang, Tengchao Lv, Lei Cui, Qifeng Chen, and Furu Wei. Textdiffuser-2: Unleashing the power of language models for text rendering. In *European Conference on Computer Vision*, pages 386–402. Springer, 2024. 1
- [13] Sixiang Chen, Jinbin Bai, Zhuoran Zhao, Tian Ye, Qingyu Shi, Donghao Zhou, Wenhao Chai, Xin Lin, Jianzong Wu, Chao Tang, et al. An empirical study of gpt-4o image generation capabilities. *arXiv preprint arXiv:2504.05979*, 2025. 2
- [14] SiXiang Chen, Jianyu Lai, Jialin Gao, Tian Ye, Haoyu Chen, Hengyu Shi, Shitong Shao, Yunlong Lin, Song Fei, Zhaohu Xing, et al. Postercraft: Rethinking high-quality aesthetic poster generation in a unified framework. *arXiv preprint arXiv:2506.10741*, 2025. 1
- [15] Jiahao Fan, Yuxin Qin, Wei Feng, Yanyin Chen, Yaoyu Li, Ao Ma, Yixiu Li, Li Zhuang, Haoyi Bian, Zheng Zhang, et al. Autopp: Towards automated product poster generation and optimization. *arXiv preprint arXiv:2512.21921*, 2025. 1
- [16] Jiasong Feng, Ao Ma, Jing Wang, Ke Cao, and Zhanjie Zhang. Fancyvideo: towards dynamic and consistent video generation via cross-frame textual guidance. In *Proceedings of the Thirty-Fourth International Joint Conference on Artificial Intelligence*, pages 10081–10089, 2025. 2
- [17] Yifan Gao, Jinpeng Lin, Min Zhou, Chuanbin Liu, Hongtao Xie, Tiezheng Ge, and Yuning Jiang. Textpainter: Multi-modal text image generation with visual-harmony and text-comprehension for poster design. In *Proceedings of the 31st ACM International Conference on Multimedia*, pages 7236–7246, 2023. 2
- [18] Yifan Gao, Zihang Lin, Chuanbin Liu, Min Zhou, Tiezheng Ge, Bo Zheng, and Hongtao Xie. Postermaker: Towards high-quality product poster generation with accurate text rendering. In *Proceedings of the Computer Vision and Pattern Recognition Conference*, pages 8083–8093, 2025. 2, 6, 7, 1
- [19] Zipeng Guo, Lichen Ma, Xiaolong Fu, Gaojing Zhou, Lan Yang, Yuchen Zhou, Linkai Liu, Yu He, Ximan Liu, Shipping Dong, et al. Repainter: Empowering e-commerce object removal via spatial-matting reinforcement learning. *arXiv preprint arXiv:2510.07721*, 2025. 1
- [20] Runze He, Bo Cheng, Yuhang Ma, Qingxiang Jia, Shanyuan Liu, Ao Ma, Xiaoyu Wu, Liebucha Wu, Dawei Leng, and Yuhui Yin. Plangen: Towards unified layout planning and image generation in auto-regressive vision language models. In *Proceedings of the IEEE/CVF International Conference on Computer Vision*, pages 18143–18154, 2025. 1
- [21] Xuanhua He, Quande Liu, Shengju Qian, Xin Wang, Tao Hu, Ke Cao, Keyu Yan, and Jie Zhang. Id-animator: Zero-shot identity-preserving human video generation. *arXiv preprint arXiv:2404.15275*, 2024. 2
- [22] Xuanhua He, Quande Liu, Zixuan Ye, Weicai Ye, Qulin Wang, Xintao Wang, Qifeng Chen, Pengfei Wan, Di Zhang, and Kun Gai. Fulldit2: Efficient in-context conditioning for video diffusion transformers. *arXiv preprint arXiv:2506.04213*, 2025. 5, 1
- [23] Zhou Hong, Rongsheng Hu, Yicheng Di, Xiaolong Xu, Ning Dong, Yihua Shao, Run Ling, Yun Wang, Juqin Wang,

- Zhanjie Zhang, et al. Stymam: A mamba-based generator for artistic style transfer. *arXiv preprint arXiv:2601.12954*, 2026. 5
- [24] Peidong Jia, Chenxuan Li, Yuhui Yuan, Zeyu Liu, Yichao Shen, Bohan Chen, Xingru Chen, Yinglin Zheng, Dong Chen, Ji Li, et al. Cole: A hierarchical generation framework for multi-layered and editable graphic design. *arXiv preprint arXiv:2311.16974*, 2023. 1
- [25] Bowen Jiang, Yuan Yuan, Xinyi Bai, Zhuoqun Hao, Alyson Yin, Yaojie Hu, Wenyu Liao, Lyle Ungar, and Camillo J Taylor. Controltext: Unlocking controllable fonts in multilingual text rendering without font annotations. *arXiv preprint arXiv:2502.10999*, 2025. 1
- [26] Zeyinzi Jiang, Chaojie Mao, Ziyuan Huang, Ao Ma, Yiliang Lv, Yujun Shen, Deli Zhao, and Jingren Zhou. Res-tuning: A flexible and efficient tuning paradigm via unbinding tuner from backbone. *Advances in Neural Information Processing Systems*, 36:42689–42716, 2023. 5
- [27] Han Jiao, Jiakai Sun, Yexing Xu, Lei Zhao, Wei Xing, and Huaizhong Lin. Mapo : Motion-aware partitioning of deformable 3d gaussian splatting for high-fidelity dynamic scene reconstruction, 2025. 5
- [28] Black Forest Labs. Flux. <https://github.com/black-forest-labs/flux>, 2024. 2, 6, 7, 8, 1
- [29] Rui Lan, Yancheng Bai, Xu Duan, Mingxing Li, Dongyang Jin, Ryan Xu, Lei Sun, and Xiangxiang Chu. Flux-text: A simple and advanced diffusion transformer baseline for scene text editing. *arXiv preprint arXiv:2505.03329*, 2025. 1
- [30] Run Ling, Ke Cao, Jian Lu, Ao Ma, Haowei Liu, Runze He, Changwei Wang, Rongtao Xu, Yihua Shao, Zhanjie Zhang, et al. Mofu: Scale-aware modulation and fourier fusion for multi-subject video generation. *arXiv preprint arXiv:2512.22310*, 2025. 1
- [31] Run Ling, Wenji Wang, Yuting Liu, Guibing Guo, Haowei Liu, Jian Lu, Quanwei Zhang, Yexing Xu, Shuo Lu, Yun Wang, et al. Ragar: retrieval augmented personalized image generation guided by recommendation. *arXiv preprint arXiv:2505.01657*, 2025. 1
- [32] Yichen Liu, Donghao Zhou, Jie Wang, Xin Gao, Guisheng Liu, Jiatong Li, Quanwei Zhang, Qiang Lyu, Lanqing Guo, Shilei Wen, et al. Hifi-inpaint: Towards high-fidelity reference-based inpainting for generating detail-preserving human-product images. *arXiv preprint arXiv:2603.02210*, 2026. 2
- [33] Zeyu Liu, Weicong Liang, Zhanhao Liang, Chong Luo, Ji Li, Gao Huang, and Yuhui Yuan. Glyph-byt5: A customized text encoder for accurate visual text rendering. In *European Conference on Computer Vision*, pages 361–377. Springer, 2024. 1
- [34] Zeyu Liu, Weicong Liang, Yiming Zhao, Bohan Chen, Lin Liang, Lijuan Wang, Ji Li, and Yuhui Yuan. Glyph-byt5-v2: A strong aesthetic baseline for accurate multilingual visual text rendering. *arXiv preprint arXiv:2406.10208*, 2024. 6, 7, 1
- [35] Runnan Lu, Yuxuan Zhang, Jiaming Liu, Haofan Wang, and Yiren Song. Easytext: Controllable diffusion transformer for multilingual text rendering. *arXiv preprint arXiv:2505.24417*, 2025. 1
- [36] Shuo Lu, Yanyin Chen, Wei Feng, Jiahao Fan, Fengheng Li, Zheng Zhang, Jingjing Lv, Junjie Shen, Ching Law, and Jian Liang. Uni-layout: Integrating human feedback in unified layout generation and evaluation. In *Proceedings of the 33rd ACM International Conference on Multimedia*, pages 7709–7718, 2025. 1
- [37] Ao Ma, Jiasong Feng, Ke Cao, Jing Wang, Yun Wang, Quanwei Zhang, and Zhanjie Zhang. Lay2story: extending diffusion transformers for layout-toggable story generation. In *Proceedings of the IEEE/CVF International Conference on Computer Vision*, pages 16102–16111, 2025. 2
- [38] Jian Ma, Yonglin Deng, Chen Chen, Nanyang Du, Haonan Lu, and Zhenyu Yang. Glyphdraw2: Automatic generation of complex glyph posters with diffusion models and large language models. In *Proceedings of the AAAI Conference on Artificial Intelligence*, pages 5955–5963, 2025. 2
- [39] Lichen Ma, Tiezhu Yue, Pei Fu, Yujie Zhong, Kai Zhou, Xiaoming Wei, and Jie Hu. Chargen: High accurate character-level visual text generation model with multimodal encoder. *arXiv preprint arXiv:2412.17225*, 2024. 1
- [40] Zhiyuan Ma, Yuzhu Zhang, Guoli Jia, Liangliang Zhao, Yichao Ma, Mingjie Ma, Gaofeng Liu, Kaiyan Zhang, Ning Ding, Jianjun Li, et al. Efficient diffusion models: A comprehensive survey from principles to practices. *IEEE Transactions on Pattern Analysis and Machine Intelligence*, 2025. 1
- [41] William Peebles and Saining Xie. Scalable diffusion models with transformers. In *Proceedings of the IEEE/CVF international conference on computer vision*, pages 4195–4205, 2023. 1
- [42] Bohao Peng, Jian Wang, Yuechen Zhang, Wenbo Li, Mingchang Yang, and Jiaya Jia. Controlnext: Powerful and efficient control for image and video generation. *arXiv preprint arXiv:2408.06070*, 2024. 1
- [43] Tianhe Ren, Shilong Liu, Ailing Zeng, Jing Lin, Kunchang Li, He Cao, Jiayu Chen, Xinyu Huang, Yukang Chen, Feng Yan, et al. Grounded sam: Assembling open-world models for diverse visual tasks. *arXiv preprint arXiv:2401.14159*, 2024. 3, 6
- [44] Robin Rombach, Andreas Blattmann, Dominik Lorenz, Patrick Esser, and Björn Ommer. High-resolution image synthesis with latent diffusion models. In *Proceedings of the IEEE/CVF conference on computer vision and pattern recognition*, pages 10684–10695, 2022. 2
- [45] Team Seedream, Yunpeng Chen, Yu Gao, Lixue Gong, Meng Guo, Qiushan Guo, Zhiyao Guo, Xiaoxia Hou, Weilin Huang, Yixuan Huang, et al. Seedream 4.0: Toward next-generation multimodal image generation. *arXiv preprint arXiv:2509.20427*, 2025. 6, 7
- [46] Gowthami Somepalli, Anubhav Gupta, Kamal Gupta, Shramay Palta, Micah Goldblum, Jonas Geiping, Abhinav Shrivastava, and Tom Goldstein. Measuring style similarity in diffusion models. *arXiv preprint arXiv:2404.01292*, 2024. 6
- [47] Quanjian Song, Xinyu Wang, Donghao Zhou, Jingyu Lin, Cunjian Chen, Yue Ma, and Xiu Li. Hero: Hierarchical extrapolation and refresh for efficient world models. *arXiv preprint arXiv:2508.17588*, 2025. 2

- [48] Quanjian Song, Donghao Zhou, Jingyu Lin, Fei Shen, Jiase Wang, Xiaowei Hu, Cunjian Chen, and Pheng-Ann Heng. Scenedecorator: Towards scene-oriented story generation with scene planning and scene consistency. *arXiv preprint arXiv:2510.22994*, 2025. 2
- [49] Wensong Song, Hong Jiang, Zongxing Yang, Ruijie Quan, and Yi Yang. Insert anything: Image insertion via in-context editing in dit. *arXiv preprint arXiv:2504.15009*, 2025. 1
- [50] Stability AI. Stablediffusion3. <https://stability.ai/news/stable-diffusion-3>, 2024. Accessed: 2024-09-03. 2
- [51] Zhenxiong Tan, Songhua Liu, Xingyi Yang, Qiaochu Xue, and Xinchao Wang. Ominicontrol: Minimal and universal control for diffusion transformer. In *Proceedings of the IEEE/CVF International Conference on Computer Vision*, pages 14940–14950, 2025. 1
- [52] Zhenxiong Tan, Qiaochu Xue, Xingyi Yang, Songhua Liu, and Xinchao Wang. Ominicontrol2: Efficient conditioning for diffusion transformers. *arXiv preprint arXiv:2503.08280*, 2025. 6, 7, 1
- [53] Yuxiang Tuo, Wangmeng Xiang, Jun-Yan He, Yifeng Geng, and Xuansong Xie. Anytext: Multilingual visual text generation and editing. *arXiv preprint arXiv:2311.03054*, 2023. 1
- [54] Yuxiang Tuo, Yifeng Geng, and Liefeng Bo. Anytext2: Visual text generation and editing with customizable attributes. *arXiv preprint arXiv:2411.15245*, 2024. 6, 7, 1
- [55] Haofan Wang, Yujia Xu, Yimeng Li, Junchen Li, Chaowei Zhang, Jing Wang, Kejia Yang, and Zhibo Chen. Rep-text: Rendering visual text via replicating. *arXiv preprint arXiv:2504.19724*, 2025. 1
- [56] Jing Wang, Ao Ma, Ke Cao, Jun Zheng, Jiasong Feng, Zhanjie Zhang, Wanyuan Pang, and Xiaodan Liang. Wisa: World simulator assistant for physics-aware text-to-video generation. In *The Thirty-ninth Annual Conference on Neural Information Processing Systems*. 2
- [57] Jing Wang, Ao Ma, Jiasong Feng, Dawei Leng, Yuhui Yin, and Xiaodan Liang. Pt-t2i/v: An efficient proxy-tokenized diffusion transformer for text-to-image/video-task. In *The Thirteenth International Conference on Learning Representations*, 2025. 2
- [58] Yun Wang, Longguang Wang, Hanyun Wang, and Yulan Guo. Spnet: Learning stereo matching with slanted plane aggregation. *IEEE Robotics and Automation Letters*, 7(3): 6258–6265, 2022. 5
- [59] Yun Wang, Longguang Wang, Kunhong Li, Yongjian Zhang, Dapeng Oliver Wu, and Yulan Guo. Cost volume aggregation in stereo matching revisited: A disparity classification perspective. *IEEE Transactions on Image Processing*, 33: 6425–6438, 2024. 1
- [60] Yun Wang, Kunhong Li, Longguang Wang, Junjie Hu, Dapeng Oliver Wu, and Yulan Guo. Adstereo: Efficient stereo matching with adaptive downsampling and disparity alignment. *IEEE Transactions on Image Processing*, 2025. 1
- [61] Yun Wang, Longguang Wang, Chenghao Zhang, Yongjian Zhang, Zhanjie Zhang, Ao Ma, Chenyou Fan, Tin Lun Lam, and Junjie Hu. Learning robust stereo matching in the wild with selective mixture-of-experts. In *Proceedings of the IEEE/CVF International Conference on Computer Vision*, pages 21276–21287, 2025. 3
- [62] Chenfei Wu, Jiahao Li, Jingren Zhou, Junyang Lin, Kaiyuan Gao, Kun Yan, Sheng-ming Yin, Shuai Bai, Xiao Xu, Yilei Chen, et al. Qwen-image technical report. *arXiv preprint arXiv:2508.02324*, 2025. 6, 7, 1
- [63] Chenfei Wu, Jiahao Li, Jingren Zhou, Junyang Lin, Kaiyuan Gao, Kun Yan, Sheng-ming Yin, Shuai Bai, Xiao Xu, Yilei Chen, et al. Qwen-image technical report. *arXiv preprint arXiv:2508.02324*, 2025. 3
- [64] Chenyuan Wu, Pengfei Zheng, Ruiran Yan, Shitao Xiao, Xin Luo, Yueze Wang, Wanli Li, Xiyan Jiang, Yexin Liu, Junjie Zhou, et al. Omnigen2: Exploration to advanced multimodal generation. *arXiv preprint arXiv:2506.18871*, 2025. 6, 7
- [65] Shaojin Wu, Mengqi Huang, Yufeng Cheng, Wenxu Wu, Ji-ah Tian, Yiming Luo, Fei Ding, and Qian He. Uso: Unified style and subject-driven generation via disentangled and reward learning. *arXiv preprint arXiv:2508.18966*, 2025. 6, 7
- [66] Shaojin Wu, Mengqi Huang, Wenxu Wu, Yufeng Cheng, Fei Ding, and Qian He. Less-to-more generalization: Unlocking more controllability by in-context generation. *arXiv preprint arXiv:2504.02160*, 2025. 1
- [67] Yu Xie, Jielei Zhang, Pengyu Chen, Ziyue Wang, Weihang Wang, Longwen Gao, Peiyi Li, Huyang Sun, Qiang Zhang, Qian Qiao, et al. Textflux: An ocr-free dit model for high-fidelity multilingual scene text synthesis. *arXiv preprint arXiv:2505.17778*, 2025. 1
- [68] Jiazheng Xu, Xiao Liu, Yuchen Wu, Yuxuan Tong, Qinkai Li, Ming Ding, Jie Tang, and Yuxiao Dong. Imagereward: Learning and evaluating human preferences for text-to-image generation. *Advances in Neural Information Processing Systems*, 36:15903–15935, 2023. 6
- [69] Yexing Xu, Longguang Wang, Minglin Chen, Sheng Ao, Li Li, and Yulan Guo. Dropouts: Dropping out gaussians for better sparse-view rendering. In *Proceedings of the Computer Vision and Pattern Recognition Conference*, pages 701–710, 2025. 5
- [70] Yukang Yang, Dongnan Gui, Yuhui Yuan, Weicong Liang, Haisong Ding, Han Hu, and Kai Chen. Glyphcontrol: Glyph conditional control for visual text generation. *Advances in Neural Information Processing Systems*, 36:44050–44066, 2023. 1
- [71] Hu Ye, Jun Zhang, Sibao Liu, Xiao Han, and Wei Yang. Ip-adapter: Text compatible image prompt adapter for text-to-image diffusion models. *arXiv preprint arXiv:2308.06721*, 2023. 1
- [72] Hui Zhang, Dexiang Hong, Maoke Yang, Yutao Cheng, Zhao Zhang, Jie Shao, Xinglong Wu, Zuxuan Wu, and Yutao Jiang. Creatidesign: A unified multi-conditional diffusion transformer for creative graphic design. *arXiv preprint arXiv:2505.19114*, 2025. 2
- [73] Lvmin Zhang, Anyi Rao, and Maneesh Agrawala. Adding conditional control to text-to-image diffusion models. In *Proceedings of the IEEE/CVF international conference on computer vision*, pages 3836–3847, 2023. 1

- [74] Yuxuan Zhang, Yirui Yuan, Yiren Song, Haofan Wang, and Jiaming Liu. Easycontrol: Adding efficient and flexible control for diffusion transformer. In *Proceedings of the IEEE/CVF International Conference on Computer Vision*, pages 19513–19524, 2025. [1](#)
- [75] Zhanjie Zhang, Quanwei Zhang, Wei Xing, Guangyuan Li, Lei Zhao, Jiakai Sun, Zehua Lan, Junsheng Luan, Yiling Huang, and Huaizhong Lin. Artbank: Artistic style transfer with pre-trained diffusion model and implicit style prompt bank. In *Proceedings of the AAAI conference on artificial intelligence*, pages 7396–7404, 2024. [2](#)
- [76] Zhanjie Zhang, Yuxiang Li, Ruichen Xia, Mengyuan Yang, Yun Wang, Lei Zhao, and Wei Xing. Lgast: Towards high-quality arbitrary style transfer with local–global style learning. *Neurocomputing*, 623:129434, 2025. [1](#)
- [77] Zhanjie Zhang, Ao Ma, Ke Cao, Jing Wang, Shanyuan Liu, Yuhang Ma, Bo Cheng, Dawei Leng, and Yuhui Yin. U-stydit: Ultra-high quality artistic style transfer using diffusion transformers. *arXiv preprint arXiv:2503.08157*, 2025. [2](#)
- [78] Zechuan Zhang, Ji Xie, Yu Lu, Zongxin Yang, and Yi Yang. In-context edit: Enabling instructional image editing with in-context generation in large scale diffusion transformer. *arXiv preprint arXiv:2504.20690*, 2025. [1](#)
- [79] Zhanjie Zhang, Quanwei Zhang, Guangyuan Li, Junsheng Luan, Mengyuan Yang, Yun Wang, and Lei Zhao. Dyartbank: Diverse artistic style transfer via pre-trained stable diffusion and dynamic style prompt artbank. *Knowledge-Based Systems*, 310:112959, 2025. [2](#)
- [80] Zhanjie Zhang, Quanwei Zhang, Junsheng Luan, Mengyuan Yang, Yun Wang, and Lei Zhao. Spast: Arbitrary style transfer with style priors via pre-trained large-scale model. *Neural Networks*, 189:107556, 2025. [2](#)
- [81] Sijie Zhao, Jing Cheng, Yaoyao Wu, Hao Xu, and Shaohui Jiao. Dreampainter: Image background inpainting for e-commerce scenarios. *arXiv preprint arXiv:2508.02155*, 2025. [1](#)
- [82] Donghao Zhou, Jiancheng Huang, Jinbin Bai, Jiaze Wang, Hao Chen, Guangyong Chen, Xiaowei Hu, and Pheng-Ann Heng. Magictailor: Component-controllable personalization in text-to-image diffusion models. *arXiv preprint arXiv:2410.13370*, 2024. [2](#)
- [83] Donghao Zhou, Jingyu Lin, Guibao Shen, Quande Liu, Jialin Gao, Lihao Liu, Lan Du, Cunjian Chen, Chi-Wing Fu, Xiaowei Hu, et al. Identitystory: Taming your identity-preserving generator for human-centric story generation. *arXiv preprint arXiv:2512.23519*, 2025. [2](#)
- [84] Yuanzhi Zhu, Jiawei Liu, Feiyu Gao, Wenyu Liu, Xinggang Wang, Peng Wang, Fei Huang, Cong Yao, and Zhibo Yang. Visual text generation in the wild. In *European Conference on Computer Vision*, pages 89–106. Springer, 2024. [1](#)

InnoAds-Composer: Efficient Condition Composition for E-Commerce Poster Generation

Supplementary Material

1. Related Work

1.1. Poster Generation

Poster generation aims to automatically produce visually appealing layouts that integrate images, text, and design elements to effectively convey information and aesthetic appeal. Recent advances such as COLE [24], Posta [9] and PosterCraft [14] leverage MLLMs to enable multi-stage control and iterative optimization, generating posters with high artistic quality and visual coherence. However, these methods are primarily designed for general or artistic compositions and are less suitable for visually appealing promotional images that must effectively present product information and attract consumer attention in e-commerce scenarios.

To address the specific requirements of e-commerce poster generation, several tailored approaches [18, 19, 81] have been proposed. DreamPainter [81] and Repainter [19] introduce inpainting-based frameworks to customize both product and background regions, enabling controlled and coherent visual synthesis. PosterMaker [18] further extends this line of work by combining prompt, subject, and text conditions to achieve fine-grained customization of background, product, and textual elements. Nonetheless, its reliance on prompt-based background generation often leads to results that deviate from desired visual or semantic constraints.

1.2. Text Rendering

Text rendering aims to generate visually coherent and legible text within images, often requiring fine-grained control over font, layout, and contextual consistency. Early text rendering methods [10, 12, 70, 84] primarily focused on generating Latin characters such as English text, but struggled to generalize to non-Latin scripts like Chinese due to the lack of corresponding text representations. To address this limitation, subsequent approaches introduced glyph-based representations [25, 33, 34, 39, 53, 54] to bridge the gap between different languages. For instance, AnyText [53] integrates glyph images as conditional inputs through a ControlNet [73] structure, enabling controllable rendering of multilingual text, while Glyph-ByT5 [33] employs a customized multilingual text encoder trained on glyph representations to generate non-Latin characters effectively.

More recent studies [3, 20, 29, 30, 35, 36, 55, 67] have adopted Diffusion Transformer (DiT) [41] architectures to achieve higher-quality and more contextually consistent text

generation. TextFlux [67], for example, uses Flux-Fill [28] as its backbone and leverages in-context learning to better capture glyph structure and spatial dependencies. Building on this line of work, FluxText [29] further explores multiple condition fusion strategies to enhance the fidelity and controllability of generated text. Inspired by these advances, we adopt a DiT-based backbone in our framework to improve the quality, clarity, and contextual alignment of text generation in e-commerce poster synthesis.

1.3. Multi-Condition Control Generation

Controllable image generation aims to incorporate multiple conditioning signals—such as text, layout, or structural guidance—into the generative process to achieve fine-grained control over visual content. Earlier approaches typically relied on ControlNet [73] or IP-Adapter [71] architectures to inject additional conditions through feature modulation or adapter networks. More recently, DiT-based methods [51, 62, 66, 74] have demonstrated strong potential for multi-condition control by integrating conditioning tokens directly into the denoising process. For example, OmniControl [51] and UNO [66] concatenate textual or semantic tokens with noisy image tokens to achieve unified conditional generation, while IC-Edit [78] and insertanything [49] performs spatial concatenation and leverages in-context learning to support diverse conditional editing tasks.

However, as the number of conditions increases, the corresponding growth in token count leads to higher attention computation costs and reduced efficiency. To mitigate this issue, several studies [1, 22, 31, 40, 42, 52, 59, 60, 76] have explored more efficient conditioning mechanisms. OmniControl2 [52], for instance, computes condition token features only once and reuses them across denoising steps, while FullDiT2 [22] introduces a dynamic token selection mechanism to adaptively identify and retain the most informative context tokens during generation. Although these methods have achieved promising results in general visual synthesis tasks, applying multi-condition control to e-commerce poster generation remains challenging, as it requires simultaneously maintaining background style consistency, accurate text rendering, and product integrity while ensuring high-quality and efficient image generation.

2. Implementation Details

InnoAds-Composer is developed based on the FLUX model [28], which is pretrained on a large-scale text rendering dataset AutoPPIM [15] and possesses an in-



Figure 8. Additional qualitative results generated by our method.

trinsic awareness of Chinese characters. The model is further optimized under tri-conditional control using our InnoComposer-80K dataset through a two-stage training strategy. (1) In *Stage I*, we fine-tune all MM-DiT blocks using LoRA modules with a rank of 256. A constant learning rate of 2×10^{-5} is adopted, and the training process requires approximately 1.1k GPU hours. (2) In *Stage II*, We removed selected tokens and fine-tuned the network to minimize performance degradation. During this stage, the learning rate was set to 1×10^{-6} , and training was conducted for approximately 100 GPU hours based on the checkpoint from *Stage I*. All training processes were conducted at a resolution of 800×800 , using Ascend 910B. During the inference phase, to ensure a fair comparison with open-source models, we used the A100 for evaluating performance and inference latency. Besides, we have supplemented the pseudocode for TFEM as follows:

3. More Experiments

More Cases. Fig. 8 presents additional generation results produced by our method. As shown, our approach not only maintains high-fidelity subject consistency for various products, but also delivers accurate and visually coherent text rendering. Moreover, the method produces realistic and diverse background styles, demonstrating its strong ability

Algorithm: Text Feature Enhancement Module (TFEM)	
Input:	Glyph image I_g , Single-glyph crops $\{C_i\}_{i=1}^N$
Output:	Enhanced glyph tokens h^c
1:	$h^{c1} \leftarrow \text{Patchify}(\text{VAE_Encode}(I_g))$ // Global structure branch
2:	for each crop C_i in $\{C_i\}_{i=1}^N$ do
3:	$f_i \leftarrow \text{OCR_Backbone}(C_i)$
4:	$p_i \leftarrow \text{Add_Positional_Encodings}(f_i, \text{abs_pos}, \text{font_size}, \text{local_pos})$
5:	end for
6:	$h^{c2} \leftarrow \text{Concat}(\{p_i\}_{i=1}^N)$ // Local semantic branch
7:	// Character Encoder Fusion via Cross-Attention
8:	$h^c \leftarrow \text{Softmax}\left(\frac{(h^{c1}W_Q)(h^{c2}W_K)^T}{\sqrt{d}}\right)(h^{c2}W_V) + h^{c1}$
9:	return LayerNorm(FFN(h^c))

Table 3. Comparison of Stage II performance under different token pruning ratios. In the pruning ratio column, [x, y, z] denote the token pruning ratios for the glyph, subject, and style conditions, respectively.

Pruning Ratio (%)	NED \uparrow	MSE \downarrow	CLIP-I \uparrow
[0,0,0]	0.976	0.056	0.582
[50,20,30]	0.971	0.057	0.581
[70,40,50]	0.970	0.057	0.562
[80,50,60] (ours)	0.969	0.058	0.594
[90,60,70]	0.582	0.066	0.451

to integrate multiple conditions into cohesive, high-quality product posters.

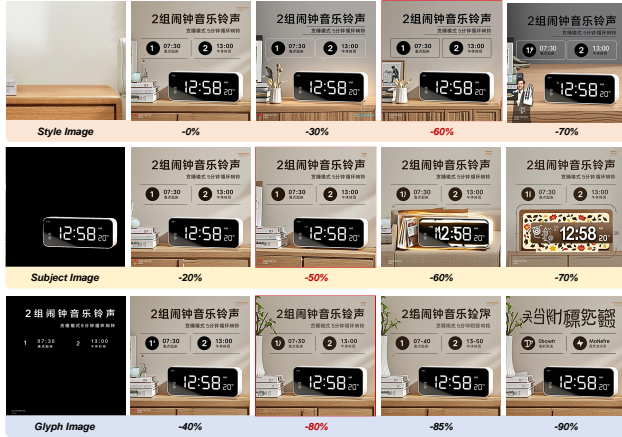


Figure 9. Qualitative results under different condition token pruning ratios.

Different Token Pruning Ratios. To validate the effectiveness of our importance-based token pruning ratios, we first evaluate alternative pruning proportions during *Stage I* inference, with qualitative results shown in Fig. 9. As illustrated, removing fewer tokens than the selected ratio preserves high-quality backgrounds, text rendering, and subject fidelity, while more aggressive pruning leads to a clear decline in generation quality. We further conduct *Stage II* training under these alternative ratios, with quantitative results summarized in Table 3. The table shows that pruning fewer tokens produces performance comparable to our chosen ratio, whereas pruning beyond it results in noticeable degradation across all metrics.